Helical Gears With Circular Arc Teeth: Simulation of Conditions of Meshing and Bearing Contact

F. L. Litvin
Chung-Biau Tsay
University of Illinois
at Chicago, IL

Abstract:

Methods proposed in this article cover: (a) generation of conjugate gear tooth surfaces with localized bearing contact; (b) derivation of equations of gear tooth surfaces; (c) simulation of conditions of meshing and bearing contact; (d) investigation of the sensitivity of gears to the errors of manufacturing and assembly (to the change of center distance and misalignment); and (e) improvement of bearing contact with the corrections of tool settings. Using this technological method we may compensate for the dislocation of the bearing contact induced by errors of manufacturing and assembly. The application of the proposed methods is illustrated by numerical examples. The derivation of the equations is given in the Appendix.

Introduction

Circular arc helical gears have been proposed by Wildhaber[10] and Novikov[8] (Wildhaber-Novikov gears). These types of gears became very popular in the sixties, and many authors in Russia, Germany, Japan and the People's Republic of China made valuable contributions to this area. The history of their researches can be the subject of a special investigation, and the authors understand that their references cover only a very small part of the bibliography on this topic.

The successful manufacturing of a new type of gearing depends on the precision of the tool used for the generation of the gears. Kudrjavzev[3] in the USSR proposed the application of two mating hobs for the generation of the W–N gears. These hobs were based on the application of two mating rack cutters, the normal section of each rack cutter representing a circular arc. Tools for the generation of circular arc helical gears have been proposed in West Germany by Winter and Looman.[11]

The circular arc helical gear is only a particular case of a general type of helical gear which can transform rotation with constant gear ratio and have a point contact at every instant. Litvin[4] and Davidov[2] simultaneously and independently proposed a method of generation for helical gears by "two rigidly connected" tool surfaces. We shall, however, limit the discussion to the case of circular arc helical gears.

The purposes of this article are twofold: the simulation of the conditions of meshing and the bearing contact for the misaligned W–N gears (the TCA method), and the adjustment of the gears for the compensation of the dislocation of the bearing contact. The main geometric properties of these gears and the method of their generation are also considered.

The tooth surfaces of circular arc helical gears (W–N gears) are in contact at a point at every instant instead of in contact along a straight line, as is the case with involute helical gears. Due to the elasticity of gear tooth surfaces, the initial contact at a point of circular arc helical gears spreads over an ellipse under the load. In the process of meshing, the center of the contacting ellipse moves over the gear tooth surface along a helix. The line of action is the set of contacting points which is represented in a fixed coordinate system rigidly connected to the frame. The line of action for the Novikov gears is a line which is parallel to the axes of rotation. The gear tooth surfaces may be generated by two rack cutters – F and P – provided with the generating surfaces Σ_F and Σ_P. We may imagine that surfaces Σ_F and Σ_P are rigidly connected to each other and are in tangency along the straight line $a - a$ (Fig. 1*a*). The normal sections of the rack cutters are two circular arcs. While the rack cutters translate with velocity **v**, the gears rotate with angular velocities $\omega^{(1)}$ and $\omega^{(2)}$, respectively. Cylinders of radii $r_1 = v \div \omega^{(1)}$ and $r_2 = v \div \omega^{(2)}$ are the gear axodes, and plane Π, which is tangent to the cylinders, is the axode of the rack cutters. The line of tangency of the axodes, $I - I$, is the instantaneous axis of rotation. Consider that the rack cutter surface Σ_F generates gear 1 tooth surface Σ_1 and Σ_P generates gear 2 tooth surfaces Σ_2. Surfaces Σ_F and Σ_1 and, correspondingly,

AUTHORS:

FAYDOR L. LITVIN *is Professor of Mechanical Engineering at the University of Illinois at Chicago. He is the author of several books and papers on gears and gearing subjects. In addition to his teaching and research responsibilities, Dr. Litvin has served as a consultant to major industrial corporations. He is Chairman of the ASME subcommittee of Gear Geometry and Manufacturing and a member of the ASME Power Transmission and Gearing Committee.*

CHANG-BIAU TSAY *did his undergraduate work at Taipei Institute of Technology, Taiwan, and earned his master's degree from Illinois Institute of Technology in Chicago. He is presently completing his doctoral work at the University of Illinois at Chicago.*

Σ_P and Σ_2, are in line contact, but Σ_1 and Σ_2 are in point contact.

Two hobs and two grinding wheels may also be used instead of two rack cutters for the generation of gears. The design of these tools is based on the idea of application of two rack cutters. The shape of these mating tools depends on the gear pitch only, and the same tools can be used for the generation of mating gears with different combinations of teeth.

Circular arc helical gears have the following advantages over involute helical gears. There are reduced contacting stresses and better conditions of lubrication. The disadvantages of these gears are higher bending stresses due to point contact of the tooth surfaces, sensitivity to the change of the center distance and to the misalignment of axes of gear rotation, and a more complicated tool shape. However, some of these disadvantages can be avoided, and circular arc helical gears may have a certain area of application. The bending stresses can be reduced by appropriate proportions of tooth elements. The effect of dislocation of the bearing contact due to the change of the distance between the gear axes may be reduced by appropriate relations between the principal curvatures of gear tooth surfaces, and may even be compensated for technologically by refinishing one of the gears (the pinion). Fortunately, the change of axes distance does not induce kinematical errors—a deviation of function $\phi_2\ (\phi_1)$ from the corresponding linear function. The misalignment of gear axes induces kinematical errors of the gear train which can exert vibrations of gears. Simultaneously, the misalignment of gear axes also effects a small dislocation of the bearing contact. The effect of misalignment of gear axes can also be compensated for technologically by refinishing of the pinion.

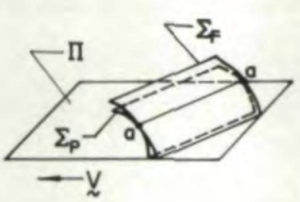

Fig. 1a

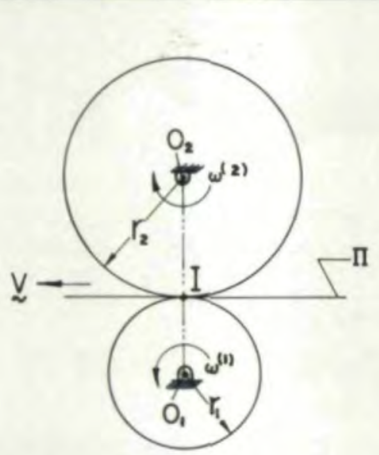

Fig. 1b

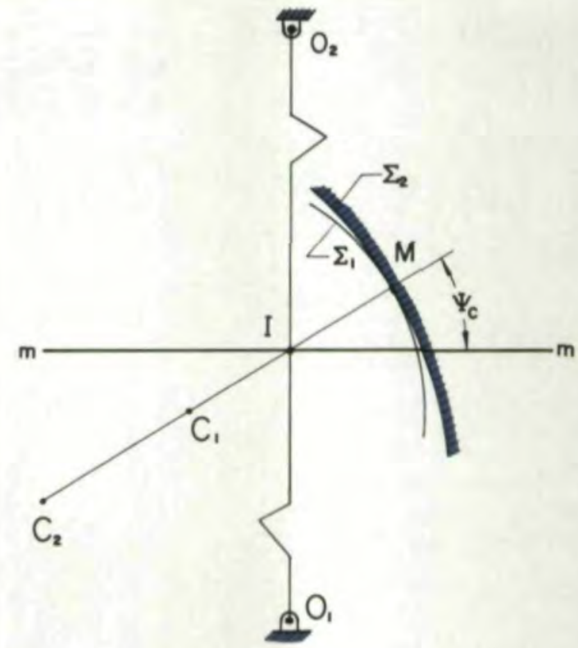

Fig. 2

The purpose of this article is to demonstrate the computer-aided simulation and adjustment of the bearing contact and conditions of meshing of circular arc helical gears.

Main Features

The main advantage of Wildhaber-Novikov gears is based on the fact that helical gears with point contact of the tooth surfaces are free of the restrictions of curvatures that are typical for spur and helical gears which have line contact of the tooth surfaces.

Consider shapes Σ_1 and Σ_2, which are the cross sections of spur or helical gears having line contact of the tooth surfaces. Shapes Σ_1 and Σ_2 are in tangency at point M (Fig. 2). The instantaneous angular velocity ratio is given by

$$m_{12} = \frac{\omega^{(1)}}{\omega^{(2)}} = \frac{0_2 I}{0_1 I} \qquad (1)$$

Generally, m_{12} is not constant and $m_{12} = f(\phi_1)$ where ϕ_1 is the angle of rotation of gear 1. It is known from the *Theory of Gearing*[5] that the derivative $dm_{12}/d\phi_1$ is equal to zero if the following equation is satisfied:

$$\frac{\varrho_2 - \varrho_1}{(\varrho_1 - l)(\varrho_2 - l)} = \frac{\Delta\varrho}{\varrho_1^2 - l(\varrho_1 + \Delta\varrho) + l^2} = \frac{r_1 + r_2}{r_1 r_2 \sin\psi_c} \qquad (2)$$

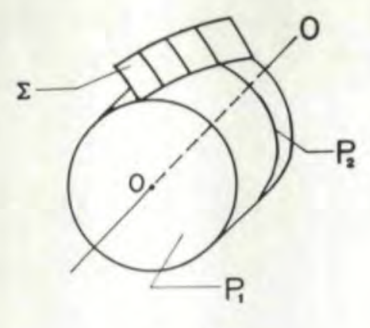

Fig. 3a

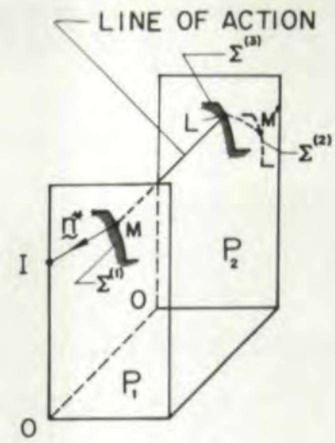

Fig. 3b

Here $\varrho_2 = C_2M$ and $\varrho_1 = C_1 M$ where C_2 and C_1 are the centers of curvatures of shapes Σ_2 and Σ_1, respectively; $\Delta\varrho = \varrho_2 - \varrho_1$; $l = IM$; $r_1 = 0_1I$ and $r_2 = 0_2I$; ψ_c is the angle formed by the shapes normal and line $m - m$.

From Equation (2) we find that the difference of curvature radii, $\Delta\varrho = \varrho_2 - \varrho_1$, depends on parameters r_1, r_2, ψ, l and ϱ_1. Thus, $\Delta\varrho$ is not a free design parameter, and it cannot be chosen as desired. Therefore, the contacting stresses cannot be reduced substantially by minimizing $\Delta\varrho$. This obstacle can be overcome if the gears are designed as helical gears provided with tooth surfaces which are in *point contact* instead of *line contact*.

Consider that the difference of curvature radii, $\Delta\varrho$, provides optimal conditions for contacting stresses, but does not satisfy Equation (2). However, the gear ratio will be constant for helical gears if their surfaces are in point contact. This statement may be proven with the following considerations.

Fig. 3*a* shows a gear tooth surface of a helical gear. Such a surface may be represented as a set of planar curves which lie in planes perpendicular to the gear axis. For instance, $\Sigma^{(1)}$ and $\Sigma^{(2)}$ are the shapes of the gear tooth surface which lie in planes P_1 and P_2, respectively (Fig. 3*a, b*). The orientation of $\Sigma^{(2)}$ is different from the orientation of $\Sigma^{(1)}$. To obtain a desired orientation for $\Sigma^{(2)}$, we have to rotate the gear through a definite angle by which point M' will come to the position L; the line ML is parallel to the axis of gear rotation.

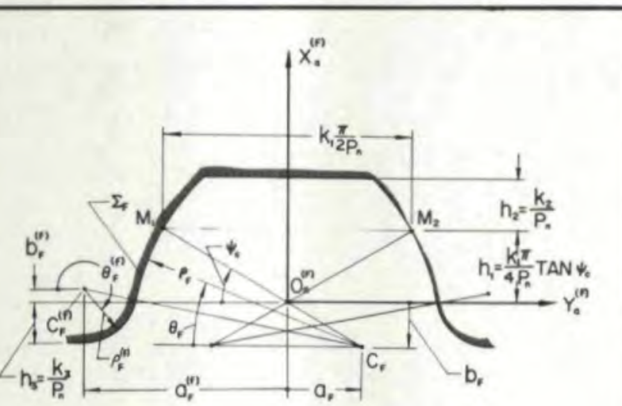

Fig. 4

Assume that initially M is the point of tangency of the mating surfaces (Fig. 3*b*). The normal $\mathbf{n}^*$ to the shape $\Sigma^{(1)}$ passes through the instantaneous center of rotation, I. The location of I on the center distance corresponds to the given gear ratio. After rotation through a definite angle, shape $\Sigma,^{(2)}$ which lies in plane P_2, will have the same orientation as that of $\Sigma,^{(1)}$ and the new point of contact of the mating surfaces will be L (Fig. 3*b*). The conditions of meshing at point L will be the same as that at point M.

We find from these considerations that helical gears which are in point contact will transform rotation with a constant gear ratio if their screw parameters h_1 and h_2 are related as follows:

$$\frac{h_1}{h_2} = \frac{\phi_1}{\phi_2} \qquad (3)$$

Here

$$h_i = r_i \tan \lambda_i \ (i = 1,2) \qquad (4)$$

where λ_i is the lead angle, and r_i is the radius of the gear axode – the pitch cylinder.

Thus, the transformation of rotation may be performed with a constant gear ratio which is independent of the curvatures of the gear tooth surfaces.

Generating Surfaces

Fig. 4 shows the normal section of the *space* of rack cutter F which generates the tooth of gear 1. The shapes of the rack cutter for each of its sides represent two circular arcs centered at C_F and $C_F^{(f)}$, respectively. The circular arc of radius $\varrho_F^{(f)}$ generates the fillet surface of the gear. Point $0_a^{(F)}$ lies in plane Π (Fig. 1).

Fig. 5 shows the normal section of the *tooth* of the rack cutter P which generates the space of gear 2. The shape of the rack cutter for each side represents two circular arcs centered at C_P and $C_P^{(f)}$, respectively. The circular arc with radius $\varrho_P^{(f)}$ generates the fillet surface of gear 2.

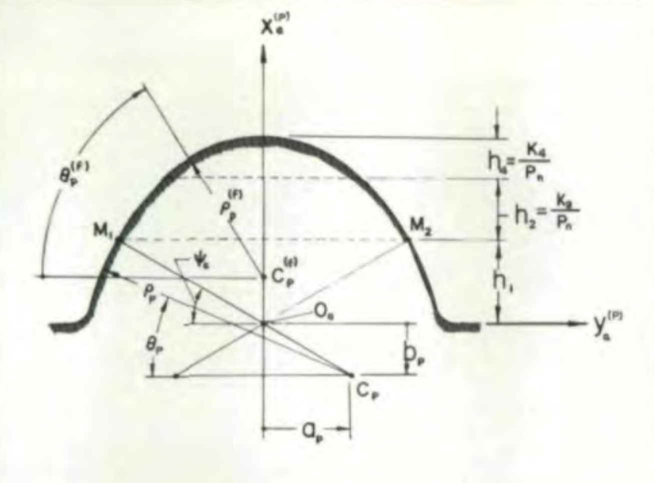

Fig. 5

The shapes of the mating rack cutters do not coincide; rather they are in tangency at points M_1 and M_2.

We may represent all four circular arcs in the coordinate systems S_a (x_a, y_a, z_a) by the same equations.

$$x_a^{(i)} = \varrho_i \sin\theta_i - b_i, \quad y_a^{(i)} = -(\varrho_i \cos\theta_i - a_i), \quad z_a^{(i)} = 0 \qquad (5)$$

Here ϱ_i is the radius of the circular arc; a_i and b_i are algebraic values which determine the location of the center of the circular arc; θ_i is the variable parameter which determines the location of a point on the circular arc (θ_i is measured clockwise from the negative axis y_a); P_n is the diametral pitch in the normal section; and ψ_c is the pressure angle. The element proportions of rack cutters h_1, h_2, h_3 and h_4 are expressed in terms of normal diametral pitch, P_n.

It was mentioned above that Equations (5) represent all four circular arcs – the shapes of both rack cutters. Thus equations

$$x_a^{(F)} = \varrho_F \sin\theta_F - b_F, \quad y_a^{(F)} = -(\varrho_F \cos\theta_F - a_F), \quad z_a^{(F)} = 0 \qquad (6)$$

represent the circular arc centered at C_F (Fig. 4).

Knowing the normal section of the rack cutter, we may derive equations of the generating surface using the matrix form of coordinate transformation. Consider that a rack cutter shape is represented in the coordinate system $S_a^{(i)}$ (Fig. 6*a*). The rack cutter surface will be generated in the coordinate system $S_c^{(i)}$ (Fig. 6*b*) while the coordinate system $S_a^{(i)}$ translates along the line $0_c^{(i)} 0_a^{(i)}$ with respect to $S_c^{(i)}$; $|0_c 0_a| = u_i$ is a variable parameter. Using the matrix equation

$$\begin{bmatrix} x_c^{(i)} \\ y_c^{(i)} \\ z_c^{(i)} \\ 1 \end{bmatrix} = \begin{bmatrix} 1 & 0 & 0 & 0 \\ 0 & \sin\lambda_i & \cos\lambda_i & u_i\cos\lambda_i \\ 0 & -\cos\lambda_i & \sin\lambda_i & u_i\sin\lambda_i \\ 0 & 0 & 0 & 1 \end{bmatrix} \begin{bmatrix} x_a^{(i)} \\ y_a^{(i)} \\ z_a^{(i)} \\ 1 \end{bmatrix} \qquad (7)$$

we obtain

$$\left.\begin{aligned} x_c^{(i)} &= \varrho_i \sin\theta_i - b_i, \\ y_c^{(i)} &= -(\varrho_i \cos\theta_i - a_i)\sin\lambda_i + u_i\cos\lambda_i \\ z_c^{(i)} &= (\varrho_i \cos\theta_i - a_i)\cos\lambda_i + u_i\sin\lambda_i \end{aligned}\right] \qquad (8)$$

In the derivation of Equations (8), we assume that $a_i > 0$ and $b_i > 0$. The unit normal to the rack cutter surface is given by the equations

$$\mathbf{n}_{(i)} = \frac{\mathbf{N}_c^{(i)}}{|\mathbf{N}_c^{(i)}|}, \quad \mathbf{N}_c^{(i)} = \frac{\partial \mathbf{r}_c^{(i)}}{\partial \theta_i} \times \frac{\partial \mathbf{r}_c^{(i)}}{\partial u_i} \qquad (9)$$

Equations (8) and (9) yield

$$[n_c^{(i)}] = \begin{bmatrix} \sin\theta_i \\ -\cos\theta_i \sin\lambda_i \\ \cos\theta_i \cos\lambda_i \end{bmatrix} \qquad (10)$$

Consider that coordinate systems $S_c^{(F)}$ and $S_c^{(P)}$ coincide. Surfaces $\Sigma_c^{(F)}$ and $\Sigma_c^{(P)}$ will be in tangency if the following equations are satisfied:

$$x_c^{(F)} = x_c^{(P)}, \quad y_c^{(F)} = y_c^{(P)}, \quad z_c^{(F)} = z_c^{(P)} \qquad (11)$$

$$n_{xc}^{(F)} = n_{xc}^{(P)}, \quad n_{yc}^{(F)} = n_{yc}^{(P)}, \quad n_{zc}^{(F)} = n_{zc}^{(P)} \qquad (12)$$

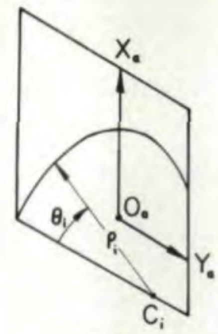

Fig. 6a

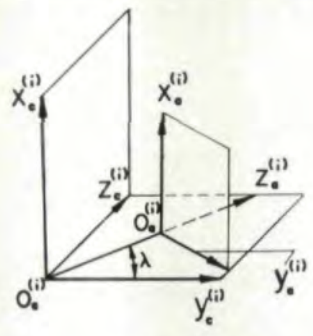

Fig. 6b

Equations (8), (10), (11), and (12) yield that surfaces Σ_F and Σ_P are in tangency along a straight line $a - a$ (Fig. 1*a*) if the following conditions are satisfied:

$$\theta_F = \theta_P = \psi_c, \quad u_F = u_P, \quad \lambda_F = \lambda_P, (\varrho_P - \varrho_F)\sin\psi_c = b_P - b_F,$$

$$(\varrho_P - \varrho_F)\cos\psi_c = a_p - a_F \tag{13}$$

Here ψ_c is the pressure angle.

The normal sections of the gear teeth do not coincide with the corresponding normal sections of the rack cutters. Neglecting the difference, we may identify the normal sections of gear teeth with the normal sections of rack cutters. The shapes of the gear teeth in the normal section are shown in Fig. 7. These shapes are in tangency at point M_1 and M_2. Considering the two sides of the teeth, we have to consider two pairs of surfaces, Σ_F and Σ_P. Each pair of these surfaces is in tangency along a straight line $a - a$ (Fig. 1*a*) and point M_i $(i = 1, 2)$ lies on $a - a$. The shape normals at M_1 and M_2 pass through point I, which lies on the instantaneous axis of rotation and coincides with the origins $0_a^{(F)}$ and $0_a^{(P)}$ for the position shown.

Gear Tooth Surfaces

Considering the generation of the gear 1 tooth surface, we use the coordinate systems $S_c^{(F)}$, S_1, and S_h, which are rigidly connected to the rack cutter *F*, gear 1, and the frame, respectively (Fig. 8*a*). Similarly, considering the generation of gear 2 tooth surface, we use coordinate systems $S_c^{(P)}$, S_2, and S_f which are rigidly connected to the rack cutter *P*, to gear 2 and to the frame, respectively. We use two different

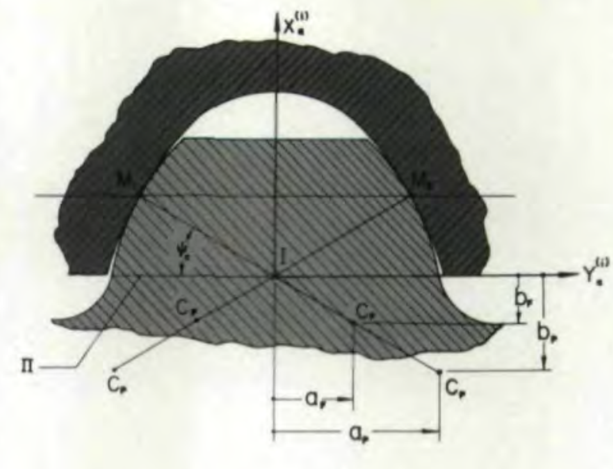

Fig. 7

fixed coordinates, S_f and S_h, to simulate various errors of assembly. Coordinate systems S_f and S_h coincide with each other if errors of gear assembly do not exist. We can simulate these errors by changing the location and orientation of the fixed coordinate system S_h with respect to S_f.

The determination of the gear tooth surface Σ_1 (Σ_1 represents gear 1 tooth surface.) is based on the following considerations. (See also the Appendix.)

Step 1: The line of contact of surfaces Σ_F *and* Σ_1 may be represented in the coordinate system $S_c^{(F)}$ as follows:[5]

$$\mathbf{r}_c^{(F)}(u_F, \theta_F) \in C^1, (u_F, \theta_F) \in A_F, \ \mathbf{N}_c^{(F)} \cdot \mathbf{v}_c^{(F1)}$$

$$= f_F(u_F, \theta_F, \phi_1) = 0 \tag{14}$$

Here u_F, θ_F are the surface coordinates of Σ_F; $\mathbf{N}_c^{(F)}$ is the surface normal; $\mathbf{v}_c^{(F1)}$ is the sliding velocity; ϕ_1 is the angle of rotation of gear 1; and A_F is the area of parameters u_F, θ_F. Equation 15,

$$f_F(u_F, \theta_F, \phi_F) = 0 \tag{15}$$

is called the equation of meshing.

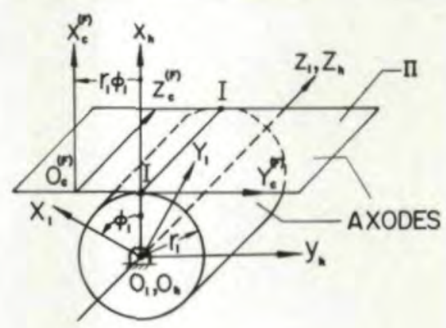

Fig. 8a

NOW A NEW HOBBER FROM MITSUBISHI, YOU CAN'T BEAT IT! COMPARE AND SEE!

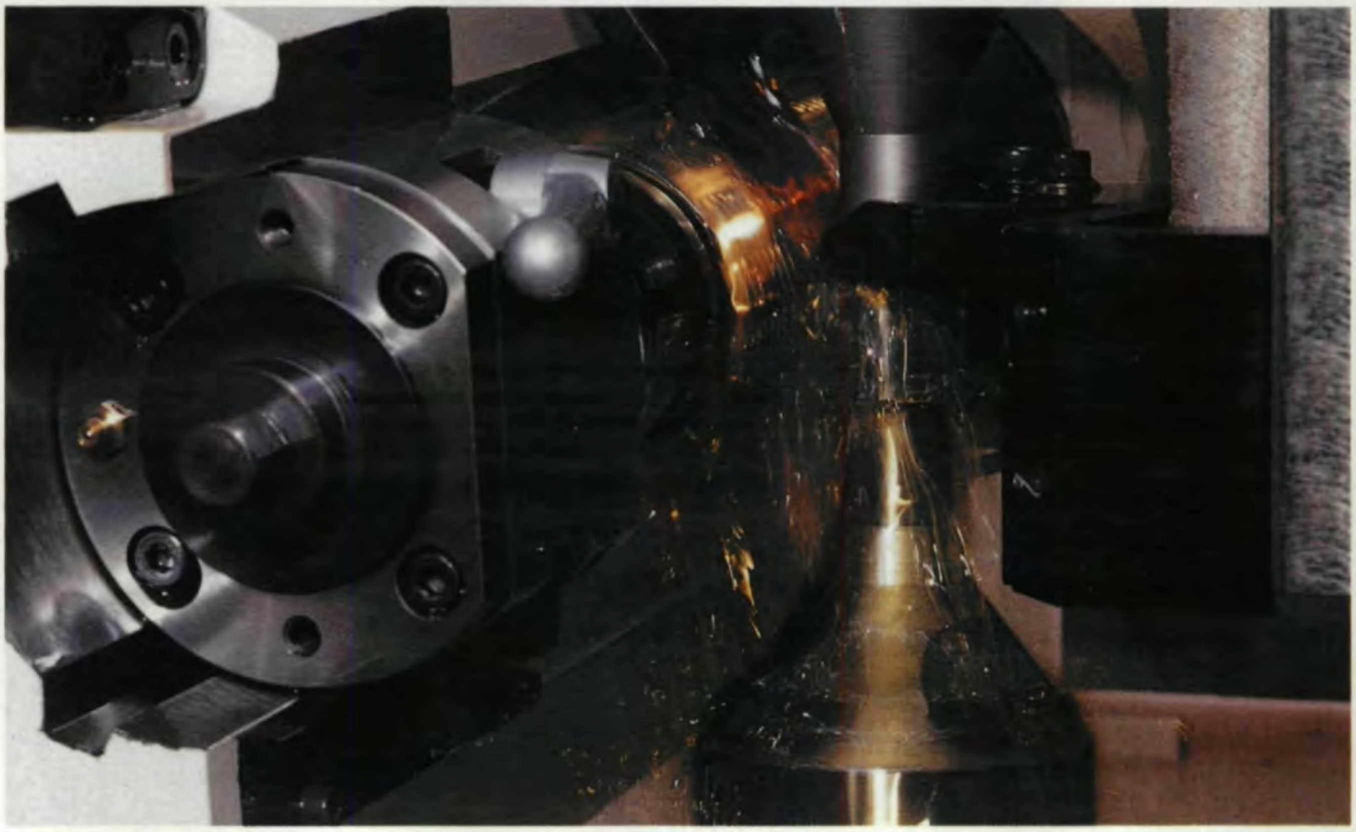

In addition to the GA-series CNC gear hobbing machines which covers a range from 10″ to 40″ diameter gears, Mitsubishi is now announcing the new high performance GA15CNC gear hobber. The GA15CNC is a 6″ machine with hob rotation of 1000rpm and table rotation of 150rpm as standard where it is an option with other manufacturers. This enables you to use multiple thread hobs to get higher production rates. Our results show that the cutting time can be reduced to about one half of the conventional machines. Needless to say, with the CNC control feature, there are no gears to change. Quick change hobs and quick change fixtures all adds up to quick changeover time. Setup time is reduced to about one third compared to conventional machines. "MENU" programming is another great feature. This relieves the operator from tedious calculations. Just input the gear and hob data. The built-in software will do all the calculations for you! You can also save floor space, hence money, with our machine. It takes only 50 sq. ft. of floor space! Compare it with the others. You'll be saving 1/2 to 3/4 of your valuable floor space! This is only the beginning! For further details, call or write us NOW!

Main Specifications

Maximum part diameter	6″, optional 8″
Maximum pitch	6DP
Maximum hob diameter	4.7″
Maximum hob length	7″
Hob shift	5″
Hob speed	150 to 1000 rpm
Hob head swivel	+/−45 deg.
Table speed	150 rpm
Main motor	7.5 hp

CNC GEAR HOBBER

GEAR EXPO '87
Booth #323

MITSUBISHI HEAVY INDUSTRIES, LTD.
5-1, Marunouchi 2-chome, Chiyoda-ku, Tokyo, Japan
Cable Address: HISHIJU TOKYO

Mitsubishi Heavy Industries America, Inc.
873 Supreme Drive, Bensenville, IL 60106 Phone: (312) 860-4220

Mitsubishi International Corporation
873 Supreme Drive, Bensenville, IL 60106 Phone: (312) 860-4222

CIRCLE A-8 ON READER REPLY CARD

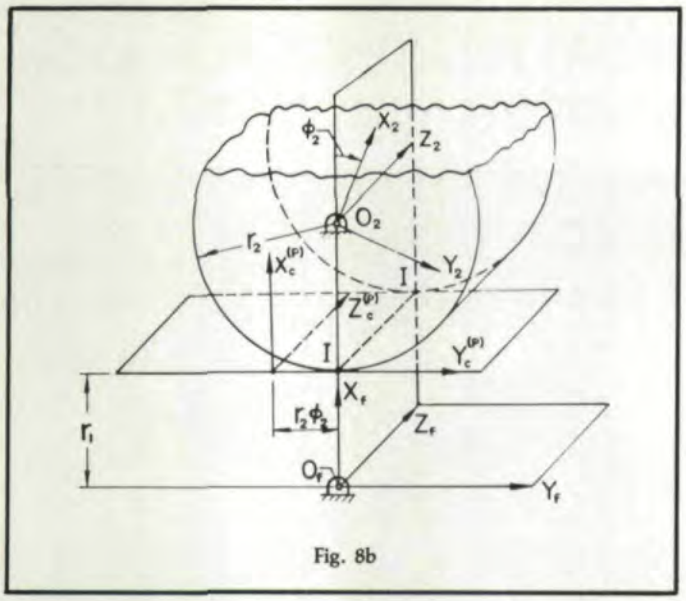

Fig. 8b

An alternative method for the determination of the equation of meshing is based on the following equations:

$$\frac{X_c^{(F)} - x_c^{(F)}}{N_{xc}^{(F)}} = \frac{Y_c^{(F)} - y_c^{(F)}}{N_{yc}^{(F)}} = \frac{Z_c^{(F)} - z_c^{(F)}}{N_{zc}^{(F)}} \tag{16}$$

Here $X_c^{(F)}$, $Y_c^{(F)}$, $Z_c^{(F)}$ are coordinates of a point on the instantaneous axis of rotation $I - I$, which is represented in $S_c^{(F)}$. $x_c^{(F)}$, $y_c^{(F)}$ and $z_c^{(F)}$ are the coordinates of a point on surface Σ_F, and $N_{xc}^{(F)}$, $N_{yc}^{(F)}$ and $N_{zc}^{(F)}$ are the direction cosines of the surface normal $\mathbf{N}_c^{(F)}$.

Step 2: The generated gear 1 tooth surface is represented in coordinate system S_1 by the following equations:

$$f_F\ (u_F,\ \theta_F,\ \phi_1) = 0,\ [r_1] = [M_{1f}]\ [M_{fc}^{(F)}]\ [r_c^{(F)}] \tag{17}$$

Here matrices $[M_{fc}^{(F)}]$ and $[M_{1f}]$ represent the coordinate transformation in transition from $S_c^{(F)}$ via S_f to S_1. The surface unit normal may be determined by the following matrix equation:

$$[n_1] = [L_1f]\ [L_{fc}^{(F)}]\ [n_c^{(F)}] \tag{18}$$

We may determine matrices $[L_{1f}]$ and $[L_{fc}^{(F)}]$ by deleting the last column and row in matrices $[M_{1f}]$ and $[M_{fc}^{(F)}]$.

Step 3: Since we will consider the mesh of gear tooth surfaces we have to represent these surfaces in a coordinate system rigidly connected to the frame. For this purpose we choose the coordinate system S_f and represent Σ_1, gear 1 tooth surface, using the following equations:

$$[r_f^{(1)}] = [M_{f1}]\ [r_1]$$

$$[n_f^{(1)}] = [L_{f1}]\ [n_1]$$

Elements of matrices $[M_{f1}]$ and $[L_{f1}]$ are expressed in terms of ϕ'_1 – the angle of rotation of gear 1, which is in mesh with gear 2. Henceforth, we will differentiate between two designations of the angle of rotation of the gears: ϕ_i is the angle of rotation of gear i in mesh with the corresponding rack cutter, and ϕ'_i is the angle of rotation of the one gear in mesh with the mating gear.

The equations of gear 2 tooth surface, Σ_2, may be determined in a similar manner. Initially, we may represent these equations in the coordinate system S_2, rigidly connected to gear 2 (Fig. 8*b*) and then in coordinate system S_f rigidly connected to the frame.

Simulations of Conditions of Meshing

We may simulate the conditions of meshing by changing the settings and orientation of the coordinate system S_h with respect to S_f. For instance, simulating the change of center distance ΔC, we may displace the origin 0_h of the coordinate system S_h by ΔC with respect to 0_f (Fig. 9*a*). Then, using the coordinate transformation from S_h to S_f we may represent the equations of surface Σ_1 and its surface normal in system S_f.

The conditions of continuous tangency of gear tooth surfaces Σ_1 and Σ_2 are represented by the following equations: [5, 6]

$$\mathbf{r}_f^{(1)}\ (\theta_F,\ \phi_1,\ \mu_1) = \mathbf{r}_f^{(2)}\ (\theta_P,\ \phi_2,\ \mu_2) \tag{19}$$

$$\mathbf{n}_f^{(1)}\ (\theta_F,\ \mu_1) = \mathbf{n}_f^{(2)}\ (\theta_P,\ \mu_2) \tag{20}$$

Equation (19) expresses that surfaces Σ_1 and Σ_2 have a common point determined with the position vectors $\mathbf{r}_f^{(1)}$ and $\mathbf{r}_f^{(2)}$. Equation (20) indicates that surfaces Σ_1 and Σ_2 have a common unit normal at their point. Equations (19) and (20), when considered simultaneously, yield a system of five independent equations only, since $|\mathbf{n}_f^{(1)}| = |n_f^{(2)}| = 1$. These five equations relate six unknowns: θ_F, ϕ_1, ϕ'_1, θ_P, ϕ_2, ϕ'_2, and thus, one of these unknowns may be considered as a variable.

Change of Axes' Distance. Equations (19), (20), (A.9-A.14) yield the following procedure for computations:

Step 1: Using equations $n_{zf}^{(1)} = n_{zf}^{(2)}$, we obtain

$$\cos\theta_F\cos\lambda_F = \cos\theta_P\cos\lambda_P \tag{21}$$

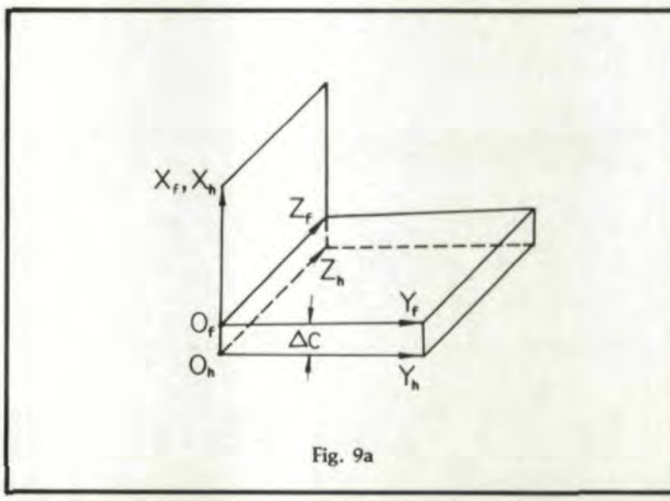

Fig. 9a

Equation (21) with $\lambda_F = \lambda_P = \lambda$ yields that

$$\theta_F = \theta_P = \theta \tag{22}$$

Step 2: Using equations $n_{yf}^{(1)} = n_{yf}^{(2)}$, $y_f^{(1)} = y_f^{(2)}$ and $x_f^{(1)} = x_f^{(2)}$, we obtain the following system of three equations in three unknowns (θ, μ_1, and μ_2):

$$\sin\theta\sin\mu_1 - \cos\theta\sin\lambda\cos\mu_1 = -\sin\theta\sin\mu_2 - \cos\theta\sin\lambda\cos\mu_2 \tag{23}$$

$$(\varrho_F\sin\theta - b_F)(\sin\theta\sin\mu_1 - \cos\theta\sin\lambda\cos\mu_1) + r_1\sin\theta\sin\mu_1 =$$

$$-(\varrho_P\sin\theta - b_P)(\sin\theta\sin\mu_2 + \cos\theta\sin\lambda\cos\mu_2) + r_2\sin\theta\sin\mu_2 \tag{24}$$

$$(\varrho_F\sin\theta - b_F)(\sin\theta\cos\mu_1 + \cos\theta\sin\lambda\sin\mu_1) + r_1\sin\theta\cos\mu_1 =$$

$$(\varrho_P\sin\theta - b_P)(\sin\theta\cos\mu_2 - \cos\theta\sin\lambda\sin\mu_2) - r_2\sin\theta\cos\mu_2 +$$

$$C'\sin\theta \tag{25}$$

Here $C' = r_1 + r_2 + \Delta C$ and ΔC is the change of center distance.

The solution to these equations for θ, μ_1 and μ_2 provides constant values whose magnitude depends on the operating center distance C' only. (The change of the center distance is ΔC). The location of the center of the contacting ellipse is determined by $\theta(\Delta C)$. Thus, the bearing contact also depends on ΔC.

We may check the solution to Equations (23), (24) and (25) using the equation $n_{xf}^{(1)} = n_{xf}^{(2)}$ which yields

$$\sin\theta\cos\mu_1 + \cos\theta\sin\lambda\sin\mu_1 = \sin\theta\cos\mu_2 - \cos\theta\sin\lambda\sin\mu_2 \tag{26}$$

Step 3: Knowing θ, we may determine the relation between parameters ϕ_1 and ϕ_2 using equation $z_f^{(1)} = z_f^{(2)}$, which yields

$$\varrho_F\cos\theta\cos\lambda - \frac{a_F}{\cos\lambda} + b_F\cot\theta\tan\lambda\sin\lambda + r_1\phi_1\tan\lambda =$$

$$\varrho_P\cos\theta\cos\lambda - \frac{a_P}{\cos\lambda} + b_P\cot\theta\tan\lambda\sin\lambda + r_2\phi_2\tan\lambda \tag{27}$$

Equation (27) provides a linear function which relates ϕ_1 and ϕ_2, since θ is constant.

Step 4: It is easy to prove that since θ, μ_1 and μ_2 have constant values, the angular velocity ratio for the gears does not depend on the center distance.

The proof is based on the following considerations: 1) Equation (27) with θ = constant, yields that $r_1 d\phi_1 = r_2 d\phi_2$ and $d\phi_1/d\phi_2 = r_2/r_1$. 2) Since $\mu_1 = \phi_1 - \phi_1'$ and $\mu_2 = \phi_2 - \phi_2'$ are constant, we obtain that $d\phi_1' = d\phi_1$, $d\phi_2' = d\phi_2$ and

$$m_{12} = \frac{\omega^{(1)}}{\omega^{(2)}} = \frac{d\phi_1'}{d\phi_2'} = \frac{r_2}{r_1} \tag{28}$$

IAD IS GEARED TO MEET YOUR MOST PRECISE MEASURING REQUIREMENTS WITH THE FETTE (PKM) INSPECTION CENTER.

IAD's Fette Inspection Center Provides .000003937 in. Positioning Accuracy.

IAD's Fette Inspection Center provides unparalleled accuracy to meet the industries' most precise measuring requirements. This IAD system is available with an exclusive software library and an Allen-Bradley CNC control that provides exact dimensional measurements of: Turbine Blades, Gear Clutch Plates, Hobs, Worm Gears, Control Cams, Double Gears, Spur Gears and more.

The highest degree of reproducibility is attained with .0001 MM accuracy. A Hewlett Packard computer with expanded graphics capability displays any deviation of involute, lead spacing, run-out, flank and more. The systems modular design allows variable applications from production line to laboratory inspection.

A patented measuring probe allows continuous probing of components. The system is capable of robotic loading and unloading allowing easy interface to automated machining cells. IAD's Fette Inspection Center is guaranteed to meet your highest measuring standards.

IAD's highly trained service engineers provide prompt service any time of the year. IAD also extends the fastest return on your investment with special terms and financing.

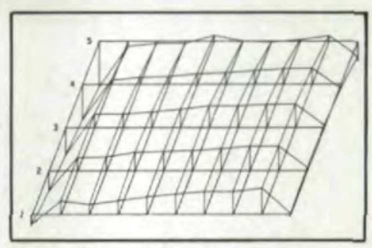

Bevel Gear Check

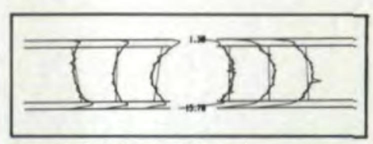

Involute Gear Check

FOR MORE INFORMATION OR APPLICATIONS ASSISTANCE, CALL OR WRITE:

IAD INCORPORATED
1307 Rankin • Troy, Mich. 48083-2828
Telephone (313) 588-2000
Telex (810) 221-5027 • Fax (313) 588-5889

CIRCLE A-16 ON READER REPLY CARD

Step 5: It is evident that since θ, μ_1 and μ_2 have constant values, the line of action of the gear tooth surfaces represents, in the fixed coordinate system S_f, a straight line which is parallel to the z_f-axis. We may determine the coordinates $x_f^{(i)}$ and $y_f^{(i)}$ $(i = 1, 2)$ of the line of action using Equations (A.9) or (A.12). (See the Appendix.) The location of the instantaneous point of contact on the line of action may be represented as a function of ϕ_1':

$$z_f^{(1)} = \varrho_F\cos\theta\cos\lambda - \frac{a_F}{\cos\lambda} + b_F\cot\theta\tan\lambda\sin\lambda + r_1\,(\mu_1+\phi_1')\tan\lambda \tag{29}$$

Step 6: We may also derive an approximate equation which relates θ and the change of the center distance, ΔC. Since μ_1 and μ_2 are small, we may make $\cos\mu_i = 1$ and $\sin\mu_i = 0$ in Equation (25). We then obtain

$$\varrho_F\sin\theta - b_F + r_1 = \varrho_P\sin\theta - b_p - r_2 + C' \tag{30}$$

where $C' = r_1 + r_2 + \Delta C$.

Equation (30) yields

$$\sin\theta = \frac{\Delta C + b_F - b_P}{\varrho_F - \varrho_P} \tag{31}$$

The nominal value of θ^0 which corresponds to the theoretical value of the center distance C, where $C = r_1 + r_2$, is given by:

$$\sin\theta^0 = \frac{b_F - b_P}{\varrho_F - \varrho_P} \tag{32}$$

Compensation for the Location of Bearing Contact Induced by ΔC. The sensitivity of the gears to the change of center distance, ΔC, may be reduced by increasing the difference $|\varrho_F - \varrho_P|$. However, this results in the increase of contacting stresses.

The dislocation of the bearing contact may be compensated for by refinishing one of the gears (preferably the pinion) with new tool settings.

Consider that θ^0 is the nominal value for the pressure angle; b_F^0 and b_P^0 ϱ_P^0 are the nominal values for the machine settings and $V\varrho_F^0$ are the nominal values for the radii of the circular arcs. These parameters are related by Equation (32). The location of the bearing contact won't be changed if the pinion is refinished with a new tool setting b_F determined as follows. (See Equation 31.)

$$\sin\theta^0 = \frac{\Delta C + b_F - b_P^0}{\varrho_F^0 - \varrho_P^0} \tag{33}$$

$$b_F = b_F^0 - \Delta C \tag{34}$$

Change of Machine Tool Settings b_F and b_P. The change of machine tool settings b_F and b_P causes: 1) the change of gear tooth thickness and backlash between the mating teeth, and 2) the dislocation of the bearing contact. The most dangerous result is the dislocation of the bearing contact.

Using similar principles of investigation, we may represent the new value of the pressure angle which corresponds to the changed machine tool settings by using the following equation:

$$\sin\theta = \frac{b_F - b_P}{\varrho_F^0 - \varrho_P^0} \tag{35}$$

Here b_F and b_P are the changed settings; $b_F \neq b_F^0$, $b_P \neq b_P^0$, where b_F^0 and b_P^0 are the nominal machine settings; $\theta \neq \theta^0$ is the new pressure angle.

We may compensate for the dislocation of the bearing contact making $\theta = \theta^0$. This can be achieved by refinishing of the pinion with a corrected setting Δb_F. Similar to Equation (33), we obtain

$$\sin\theta^0 = \frac{b_F - b_P^0 + \Delta b_F}{\varrho_F^0 - \varrho_P^0} \tag{36}$$

Misalignment of Axes of Gear Rotation. Consider that the axis of gear 1 rotation is not parallel to the axis of gear 2 rotation and forms an angle $\Delta\gamma$ (Fig. 9*b*). The coordinate transformation from S_h to S_f is represented by the matrix equations

$$[r_f^{(1)}] = [M_{fh}][r_h^{(1)}], [n_f^{(1)}] = [L_{fh}][n_h^{(1)}] \tag{37}$$

Using Equations (37), (A.9-A.14) (19) and (20), we may represent the tangency of surfaces Σ_1 and Σ_2 for misaligned gears as follows:

$$A_2\cos\mu_2 - B_2\sin\mu_2 + C = A_1\cos\mu_1 + B_1\sin\mu_1 \tag{38}$$

$$-A_2\sin\mu_2 - B_2\cos\mu_2 = (A_1\sin\mu_1 - B_1\cos\mu_1)\cos\Delta\gamma + \left(\varrho_F\cos\theta_F\cos\lambda_F - \frac{a_F}{\cos\lambda_F} + b_F\cot\theta_F\tan\lambda_F\sin\lambda_F + r_1\phi_1\tan\lambda_F\right)\sin\Delta\gamma \tag{39}$$

(See Equations (A.11) and (A.14) in the Appendix.)

$$\varrho_P\cos\theta_P\cos\lambda_P - \frac{a_P}{\cos\lambda_P} + b_P\cot\theta_P\sin\lambda_P\tan\lambda_P + r_2\phi_2\tan\lambda_P = -(A_1\sin\mu_1 - B_1\cos\mu_1)\sin\Delta\gamma + \left(\varrho_F\cos\theta_F\cos_F - \frac{a_F}{\cos\lambda_F} + b_F\cot\theta_F\tan\lambda_F\sin\lambda_F + r_1\phi_1\tan\lambda_F\right)\cos\Delta\gamma \tag{40}$$

$$\sin\theta_P\cos\mu_2 - \cos\theta_P\sin\lambda_P\sin\mu_2 = \sin\theta_F\cos\mu_1 + \cos\theta_F\sin\lambda_F\sin\mu_1 \tag{41}$$

$$-\sin\theta_P\sin\mu_2 - \cos\theta_P\sin\lambda_P\cos\mu_2 - = (\sin\theta_F\sin\mu_1 - \cos\theta_F\sin\lambda_F\cos\mu_1)\cos\Delta\gamma + \cos\theta_F\cos\lambda_F\sin\Delta\gamma \tag{42}$$

$$\cos\theta_P\cos\lambda_P = -(\sin\theta_F\sin\mu_1 - \cos\theta_F\sin\lambda_F\cos\mu_1)\sin\Delta\gamma + \cos\theta_F\cos\lambda_F\cos\Delta\gamma \tag{43}$$

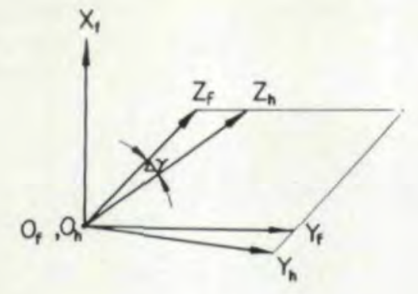

Fig. 9b

Equations (38-43) form a system of five independent equations in six unknowns: θ_P, θ_F, μ_1 μ_2, ϕ_1 and ϕ_2. We may remind readers that only two equations from equation system (41-43) are independent since $|\mathbf{n}_f^{(1)}| = 1$ and $|\mathbf{n}_f^{(2)}| = 1$.

The computational procedure is as follows: 1) We consider equations (38), (39), (42) and (43) which form a system of four equations in five unknowns: θ_F, θ_P, μ_1, μ_2 and ϕ_1. Fixing in ϕ_1 we may obtain the solutions by $\theta_F(\phi_1)$, $\theta_P(\phi_1)$, $\mu_1(\phi_1)$ and $\mu_2(\phi_1)$. 2) Using Equation (40) we obtain $\phi_2(\phi_1)$. 3) Then, using the equations

$$\phi_1' = \phi_1 - \mu_1, \quad \phi_2' = \phi_2 - \mu_2 \tag{44}$$

we can obtain the relation between the angles ϕ_2' and ϕ_1' of gear rotation. Function $\phi_2'(\phi_1')$ is a nonlinear function and its deviation from the linear function is given by

$$\Delta\phi_2'(\phi_1') = \phi_2'(\phi_1') - \frac{N_1}{N_2}\phi_1' \tag{45}$$

Here $\Delta\phi_2'(\phi_1')$ represents the kinematical errors of the gear train and $\phi_F(\phi_1')$ and $\theta_P(\phi_1')$ represent the change of location of the bearing contact induced by the misalignment of gear axes.

Compensation for the Location of Bearing Contact Induced by the Gear Misalignment. The dislocation of the bearing contact induced by misalignment of the axes of gear rotation may be compensated for by the change of the lead angle λ_F (or λ_P). This can be done technologically by refinishing of the pinion.

Example 1: The Influence of Change of Axes Distance. Given the rack parameters shown in Figs. 4 and 5: tooth numbers, $N_1 = 12$, $N_2 = 94$; the lead angle $\lambda_F = \lambda_P = 75°$; the nominal pressure angle $\theta^0 = 30°$; the normal diametral pitch $P_n = 2$; the nominal axes distance $C = 29.239515''$ and the change of axes distance, $\Delta C = 0.021''$. Due to the change of axes distance, the new value of the pressure angle θ is: 1) $\theta = 12.81412$ deg (exact solution provided by equation system (23-25); 2) $\theta = 12.70903$ deg (approximate solution provided by Equation 31).

The compensation for the dislocation of bearing contact is achieved by the new machine setting $b_F = -0.021$ in. which provides $\theta = \theta^0 = 30$ deg although $C = C0 + \Delta C$.

Example 2: The Influence of Misalignment of Gear Axes. The nominal rack and gear parameters are the same as shown in Example 1. The misalignment is given by $\Delta\gamma = 0.1$ deg (Fig. 9). The kinematical errors $\Delta\phi_2'$ and the change of θ_F and θ_P are given in Table 1.

Table 1 Kinematical errors

No.	ϕ_1	θ_F	θ_P	$\Delta\phi_2'$ (in s)
1	−20 deg	32.2520 deg	31.6521 deg	59.88 in.
2	−10 deg	32.2527 deg	31.6528 deg	29.94 in.
3	0 deg	32.2531 deg	31.6531 deg	0.00 in.
4	10 deg	32.2530 deg	31.6530 deg	−29.94 in.
5	20 deg	32.2526 deg	31.6526 deg	−59.89 in.

The compensation of kinematical errors is achieved with the change of the lead angle of the pinion $\lambda_F = 75.093$ deg ($\Delta\lambda_F = 0.093$ deg). The kinematical errors after compensation are given in Table 2.

Using the proposed method of compensation we could reduce substantially the kinematical errors induced by the misalignment of axes of gear rotation by approximately 250 times.

Conclusion

The authors have considered the geometric properties of circular arc helical gears and the method of their generation.

Table 2 Compensated kinematical errors

No.	ϕ_1	θ_F	θ_P	$\Delta\phi_2'$ (in s)
1	−20 deg	30.1892 deg	30.1440 deg	0.23 in.
2	−10 deg	30.1900 deg	30.1449 deg	0.12 in.
3	0 deg	30.1905 deg	30.1452 deg	0.00 in.
4	10 deg	30.1904 deg	30.1452 deg	−0.12 in.
5	20 deg	30.1900 deg	30.1447 deg	−0.24 in.

A method for the simulation of the conditions of meshing and the bearing contact has been proposed. Using this method the sensitivity of the gears to the change of center distance and to the misalignment of gears has been investigated. A technological method for the improvement of the bearing contact for misaligned gears has been proposed. The presented numerical examples illustrate the influence of the abovementioned errors and the method for compensation of the dislocation of the bearing contact.

References

1. CHIRONIS, N. P. "Design of Novikov Gears." *Gear Design and Application*, N. P. Chironis (Ed.), McGraw-Hill, New York.
2. DAVIDOV, J. S. "The Generation of Conjugate Surfaces by Two Rigidly Connected Tool Surfaces," *Vestnik Mashinostroyenia*, 1963, No. 2.
3. KUDRJAVZEV, V. N. *Epicycloidal Trains*, Mashgis, 1966.
4. LITVIN, F. L., "The Investigation of the Geometric Properties of a Variety of Novikov Gearing," *The Proceedings of Leningrad Mechanical Institute*, 1962, No. 24 (in Russian).
5. LITVIN, F. L., *Theory of Gearing*, 2nd edition, Nauka, 1968 (in Russian). New edition (in English), revised and completed, sponsored by NASA, is in press.
6. LITVIN, F. L., RAHMAN, P., and GOLDRICH, R. N., "Mathematical Models for the Synthesis and Optimization of Spiral Bevel Gear Tooth Surfaces," NASA Contractor Report 3553, 1982.
7. NIEMANN, G., "Novikov Gear System and Other Special Gear Systems for High Load Carrying Capacity," *VDI Berichte*, No. 47, 1961.
8. NOVIKOV, M. L., USSR Patent No. 109, 750, 1956.
9. WELLS, C. F., and SHOTTER, B. A., "The Development of 'Circarc' Gearing, *AEI Engineering*, March-April, 1962.
10. WILDHABER, E., US Patent, No. 1,601,750 issued Oct. 5, 1926, and "Gears with Circular Tooth Profile Similar to the Novikov System," *VDI Berichte*, No. 47, 1961.
11. WINTER, H., and LOOMAN, J., "Tools for Making Helical Circular Arc Spur Gears," *VDI Berichte*, No. 47, 1961.

APPENDIX

Gear Tooth Surfaces

Gear 1 Tooth Surface. Substituting subscript i for F in Equations (8) and (10) and taking into account that $b_F > 0$, we obtain:

$$[r_c^{(F)}] = \begin{bmatrix} \varrho_F\sin\theta_F - b_F \\ (\varrho_F\cos\theta_F - a_F)\cos\lambda_F + u_F\sin\lambda_F \\ 1 \end{bmatrix} \quad (A.1)$$

$$[n_c^{(F)}] = \begin{bmatrix} \sin\theta_F \\ -\cos\theta_F\sin\lambda_F \\ \cos\theta_F\cos\lambda_F \end{bmatrix} \quad (A.2)$$

Equations (A.1) and (A.2) represent the generating surface Σ_F and the unit normal to this surface. We may derive the equation of meshing using equations (A.1), (A.2) and (16) with

$$X_c^{(F)} = 0, \quad Y_c^{(F)} = r_1\phi_1, \quad Z_c^{(F)} = l \quad (A.3)$$

where $X_c^{(F)}$, $Y_c^{(F)}$ and $Z_c^{(F)}$ are coordinates of the point of intersection of the normal to Σ_F and the instantaneous axis of rotation, I-I (Fig. 8*a*). We then obtain

$$f_F(u_F,\theta_F,\phi_1) = (r_1\theta_1 - u_F\cos\lambda_F - a_F\sin\lambda_F)\sin\theta_F + b_F\cos\theta_F\sin\lambda_F = 0 \quad (A.4)$$

Equation of meshing (A.4) yields

$$u_F = \frac{r_1\phi_1 - a_F\sin\lambda_F}{\cos\lambda_F} + b_F\cot\theta_F\tan\lambda_F \quad (A.5)$$

Equations (A.1) and (A.5), when considered simultaneously, represent a family of contacting lines on surface Σ_F. Eliminating u_F, we may represent this family of lines of contact as follows:

$$\begin{bmatrix} x_c^{(F)} \\ y_c^{(F)} \\ z_c^{(F)} \\ 1 \end{bmatrix} = \begin{bmatrix} \varrho_F\sin\theta_F - b_F \\ -(\varrho_F\sin\theta_F - b_F)\cot\theta_F\sin\lambda_F + r_1\phi_1 \\ (\varrho_F\sin\theta_F + b_F\tan^2\lambda_F)\cot\theta_F\cos\lambda_F - \dfrac{a_F}{\cos\lambda_F} + r_1\phi_1\tan\lambda_F \\ 1 \end{bmatrix} \quad (A.6)$$

Using Equations (A.6) and the coordinate transformation from $S_c^{(F)}$ to S_1 we obtain

$$\begin{aligned} x_1 &= (\varrho_F\sin\theta_F - b_F + r_1)\cos\phi_1 + (r_F\cos\theta_F - b_F\cot\theta_F)\sin\phi_1\sin\lambda_F \\ y_1 &= (\varrho_F\sin\theta_F - b_F + r_1)\sin\phi_1 - (\varrho_F\cos\theta_F - b_F\cot\theta_F)\cos\phi_1\sin\lambda_F \\ z_1 &= \varrho_F\cos\theta_F\cos\lambda_F - \frac{a_F}{\cos\lambda_F} + b_F\cot\theta_F\tan\lambda_F\sin\lambda_F + r_1\phi_1\tan\lambda_F \end{aligned} \quad \text{(A.7)}$$

The surface unit normal is given by

$$[n_1] = \begin{bmatrix} \sin\theta_F\cos\phi_1 + \cos\theta_F\sin\lambda_F\sin\phi_1 \\ \sin\theta_F\sin\phi_1 - \cos\theta_F\sin\lambda_F\cos\phi_1 \\ \cos\theta_F\cos\lambda_F \end{bmatrix} \quad \text{(A.8)}$$

Using the coordinate transformation from S_1 to S_h we obtain

$$\left.\begin{aligned} x_h^{(1)} &= A_1\cos\mu_1 + B_1\sin\mu_1 \\ y_h^{(1)} &= A_1\sin\mu_1 - B_1\cos\mu_1 \\ z_h^{(1)} &= \varrho_F\cos\theta_F\cos\lambda_F - \frac{a_F}{\cos\lambda_F} + b_F\cot\theta_F\tan\lambda_F\sin\lambda_F + r_1\phi_1\tan\lambda_F \end{aligned}\right] \quad \text{(A.9)}$$

$$[n_h^{(1)}] = \begin{bmatrix} \sin\theta_F\cos\mu_1 + \cos\theta_F\sin\lambda_F\sin\mu_1 \\ \sin\theta_F\sin\mu_1 - \cos\theta_F\sin\lambda_F\cos\mu_1 \\ \cos\theta_F\cos\lambda_F \end{bmatrix} \quad \text{(A.10)}$$

Here

$$A_1(\theta_F) = \varrho_F\sin\theta_F - b_F + r_1, \quad B_1(\theta_F) = (\varrho_F\cos\theta_F - b_F\cot\theta_F)\sin\lambda_F, \text{ and } \mu_1 = \phi_1 - \phi_1' \quad \text{(A.11)}$$

Equations (A.9) and (A.10) with a fixed value for ϕ_1', represent in the coordinate system S_h, surface Σ_1 and the unit normal to Σ_1. These equations with different values for ϕ_1', represent in S_h, a *family* of surfaces Σ_1 and the unit normals to these surfaces.

The derivation of equations for gear 2 surface Σ_2 and its unit normal is based on similar considerations. We may represent these equations in S_f as follows:

$$\left.\begin{aligned} x_f^{(2)} &= A_2\cos\mu_2 - B_2\sin\mu_2 + C \\ y_f^{(2)} &= -A_2\sin\mu_2 - B_2\cos\mu_2 \\ z_f^{(2)} &= \varrho_P\cos\theta_P\cos\lambda_P - \frac{a_P}{\cos\lambda_P} + b_P\cot\theta_P\sin\lambda_P\tan\lambda_P + r_2\phi_2\tan\lambda_P \end{aligned}\right] \quad \text{(A.12)}$$

$$[n_f^{(1)})] = \begin{bmatrix} \sin\theta_P\cos\mu_2 + \cos\theta_P\sin\lambda_P\sin\mu_2 \\ -\sin\theta_P\sin\mu_2 - \cos\theta_P\sin\lambda_P\cos\mu_2 \\ \cos\theta_P\cos\lambda_P \end{bmatrix} \quad \text{(A.13)}$$

Here

$$A_2(\theta_P) = \varrho_P\sin\theta_P - b_P - r_2, \quad B_2(\theta_P) = (\varrho_P\cos\theta_P - b_P\cot\theta_P)\sin\lambda_P, \text{ and } \mu_2 = \phi_2 - \phi_2' \quad \text{(A.14)}$$

The nominal value of the center distance is $C = r_1 + r_2$.

Acknowledgement: Originally published in *Journal of Mechanisms, Transmission and Automation in Design*, Dec., 1985. Reprinted with permission of American Society of Mechanical Engineers. Paper No. 84-DET-175.